AN APPROACH TO ASSESS AIRFRAME WEIGHT REDUCTION PERFORMANCE OF STITCHED COMPOSITE TECHNOLOGIES

Jason A. Corman* , **Dimitri N. Mavris***
***Georgia Institute of Technology**

Keywords: *Stitched Composites, PRSEUS, Structural Weight Estimation, Conceptual Aircraft Design, Aircraft Technology Performance*

Abstract

An approach is presented for assessing performance of stitched, resin-infused (S/RI) composite airframe technologies. This method considers both direct and enabling effects of the technologies to reduce structural weight early in the conceptual phase of aircraft design. Weight reduction estimates are provided for a S/RI composite technology applied to a hybrid wing body (HWB) aircraft. These estimates are found as a function of: 1) conceptual phase design variables that define the shape, or outer mold line (OML), of the aircraft, 2) structural layout design variables to account for design uncertainty, and 3) updated structural properties that result from physical experimentation.

1 Introduction

As design in the aircraft industry pushes the boundaries of current capabilities, evolutionary and revolutionary concepts and technologies are investigated to meet market and regulating demands of cost, performance, and safety. The HWB was shown to be an appropriate candidate for improvements in performance and operating costs through the U.S. FAA Continuous Low Energy, Emissions, and Noise (CLEEN [14]) and NASA Environmentally Responsible Aviation (ERA [2]) programs [17]. This configuration, however, is outside the scope of traditional conceptual design models that are empirically built with historical production data, especially for airframe weight. Therefore, aircraft performance estimates are made with a higher level of uncertainty and risk, and airframe weight estimation must be implemented through alternative methods.

Comparative improvements for the commercial HWB configuration over traditional tube-and-wing (T&W) aircraft were supported by predicted superiority in aerodynamic efficiency (L/D) [10]. However, internal pressurization of the cabin section for the HWB presented structural challenges for its non-circular cross-section. For example, traditional structural concepts would potentially need to be over-sized in the skin of the HWB centerbody cabin section to prevent fatigue of cyclic pressurization while withstanding combined bending loads from: 1) lift on the outboard wings and 2) internal pressure acting on a relatively flat surface. The resulting increased structural weight could counteract the improvements in aerodynamic efficiency, which justified the need for an appropriate structural technology. Trades to assess the feasibility and viability of a commercial HWB configuration as well as the enabling impact of a structural technology should be made in the early conceptual design phase. Therefore, a process is needed that estimates structural technology performance that considers the effect of conceptual phase vehicle design variables. The following sections describe an approach to characterize the perfor-

mance of a structural technology in the context of aircraft structural weight reduction.

2 Structural Technology Performance of Stitched Composites

One of the major benefits of current state of the art (SoA) composites for airframe manufacturing is the ability to co-cure stiffened, thin shelled structural configurations. Co-curing alleviates the need for rivets and other fasteners, which can significantly reduce structural weight. The drawback to this configuration, however, is its inability to arrest damage propagation, effectively removing the tear strap implemented between the thin wall and stiffeners in metallic constructed aircraft. Therefore, delamination as a result of HWB centerbody out-of-plane loads is a critical failure mode of SoA aircraft composites.

2.1 PRSEUS Characteristics

A proposed solution for the commercial HWB centerbody was a structural technology in the class of stitched, resin-infused (S/RI) composites: the Pultruded Rod Stitched Efficient Unitized Structures (PRSEUS), shown in Fig. 1. This breakthrough in manufacturing leverages stitching as a mechanism of damage arrestment and can therefore use a damage tolerant design philosophy rather than the safe-life philosophy required of SoA composites [3]. It also addressed other concerns of traditional composites, such as fastener pull-through and debonding.

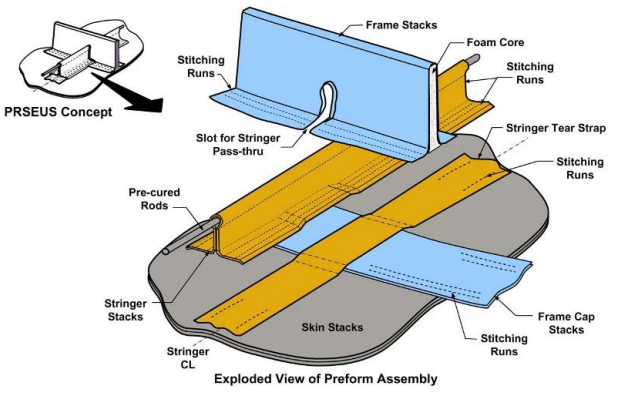

Fig. 1 PRSEUS attributes [19]

The following describe PRSEUS technology features and how they contribute to estimated structural weight reduction.

Stitching and Unitization Composite stitching enables progressive local failures, shifting of load paths, and suppression of delamination and laminate pull-off failure modes, which are all mechanisms that contribute to structural weight reduction [6]. Additionally, unitization of the PRSEUS structural configurations enables continuous load paths at stiffener-to-stiffener interfaces with decreased stress concentrations while also decreasing the number of fasteners required for assembly [19]. A unitized and stitched stiffener construction also creates a panel that can operate locally in the post-buckling regime. Therefore, local skin buckling is no longer a means of critical failure since the load is transmitted efficiently through the stiffeners [7, 1].

Warp-Knit Fabric and CAPRI Carbon fiber composite materials have much higher stiffness-to-density and strength-to-density ratios and are less prone to fatigue compared to conventional aluminum aircraft materials [15]. These attributes, without other considerations of the design process, allows for more weight efficient design. Therefore, composite construction that behaves like damage arresting conventional aluminum construction takes full advantage of these better performing ratios. The design of the warp-knit fabric enables stitching and the benefits associated with it, and the controlled atmospheric pressure resin infusion (CAPRI) process eliminates the need for autoclave curing. Without the need for an autoclave, much larger panels can be fabricated, which saves weight through decreasing the number of required panel joints, and a reduction of manufacturing costs can also be achieved [19].

Foam Core Frame The frame acts similar to

a hat stiffener, increasing the moment of inertia of the cross section to counteract bending. A foam core is used for both manufacturing and performance functionality. The foam expands during cure, providing an inner surface to contain resin and maintain shape. A secondary function is to provide stability to the frame web by resisting inward deflections during loading.

Rod Stringer The rod stringer provides significant bending stiffness compared to traditional integral blade stiffeners or J-stiffeners. Its pultruded rod is dominated by 0-degree fibers to increase stiffness and strength in the stringer direction, and the pultrusion process ensures straightness of the rod to aid in stability by maintaining stringer shape.

These characteristics all provide detailed structural information as to why a stitched, resin-infused composite may be more structurally efficient; however, they offer little insight into the actual structural weight reduction that can be achieved through PRSEUS implementation. A transfer function is needed that connects structure details to this performance metric, which is described next.

2.2 Performance Estimation

To ensure consistency with conceptual design models, technology performance at the aircraft level is tied to the aircraft structural weight. Characterization of this performance, i.e. structural weight reduction, requires a basis of comparison for the technology. The baseline for comparison is an important definition because it also must be consistent with conceptual design models, especially empirical models built from historical data like NASA's Flight Optimization System (FLOPS) [12]. The following convention for aircraft level structural technology performance is defined as a weight reduction:

$$\Delta W_S = W_{S,B} - W_{S,T} \tag{1}$$

where $W_{S,B}$ is the airframe structural weight of an aircraft implemented with baseline structure, and $W_{S,T}$ is the airframe weight of an aircraft implemented with the technology. This convention was used so that "increased performance" could be denoted as an increase to the value for ΔW_S, and therefore, positive values of performance denote a decrease in structural weight.

Implementation of performance impact in conceptual design is defined as a scale factor on weight, or:

$$k_{ST} = 1 - \frac{\Delta W_S}{W_{S,B}} = \frac{W_{S,T}}{W_{S,B}} \tag{2}$$

In FLOPS, historical data points for traditional T&W aircraft regression models encompass airframes that were built with some type of thin-shelled skin-stiffened aluminum. Therefore, proper definition of baselines is important to avoid potential mishaps in bookkeeping. For example, consider a scenario in which the baseline chosen for higher fidelity technology performance estimation was a different composite structure, which was the case in the benchmark PRSEUS performance estimation study [19]. However, the conceptual design model was generated with data from aluminum-based aircraft configurations. In this case, technology performance is defined as:

$$\begin{aligned} \Delta W_{S,total} &= W_{S,CD} - W_{S,T} \\ &= (W_{S,CD} - W_{S,B}) + (W_{S,B} - W_{S,T}) \\ &= \Delta W_{S,B} + \Delta W_{S,T} \end{aligned} \tag{3}$$

where $W_{S,CD}$ is the structural weight estimated by the traditional conceptual design model, and $\Delta W_{S,B}$ represents performance of the composite baseline over the aluminum "baseline" in the traditional conceptual design model.

If structural technology performance is to be characterized for conceptual design, there are other factors that contribute to the potential weight reduction. For instance, variation in outer mold line (OML) or structural layout (SL) for a given aircraft could lead to variation in structural weight due to: external aerodynamic load distributions, fuel distribution, internal load paths, etc. If the variation in structural weight $(\partial W_S/\partial \mathbf{X})$ is

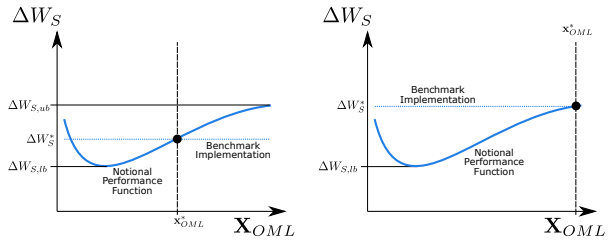

Fig. 2 Potential for error in technology performance in a scalar vs. functional approach

different for the baseline structure and the technology, then by definition, performance would vary throughout the design space, $\mathbf{X}$.

Figure 2 shows the potentially incorrect estimation of technology performance if a scalar characterization is performed, i.e. for a single baseline outer mold line $\left(\mathbf{X}^*_{OML}\right)$, rather than a functional characterization throughout the OML design space. A similar phenomena could occur in the structural layout design space $\left(\mathbf{X}^*_{SL}\right)$. The research presented in this paper describes a methodology for a complete, traceable characterization of an S/RI composite technology, including effects of the design space itself. This approach also provides insights to the probability of error in performance estimation when comparing a functional versus baseline scalar performance estimation technique.

3 Approach for Performance Estimation

Obtaining traceable estimates of structural technology performance as a function of the design spaces mentioned in the previous section requires more advanced structural weight estimation techniques than empirical models built from historical data. Physics-based weight estimation was used in the benchmark approach for scalar characterization of PRSEUS weight reduction performance [19]. The global-local approach described by Velicki considers a single baseline aircraft structural model to which assessments in technology performance are made. Achievement of ΔW_S estimation as a function of the OML and SL design spaces is critically enabled by a fully parametric finite element modeling framework, like that described in Refs. [9, 5].

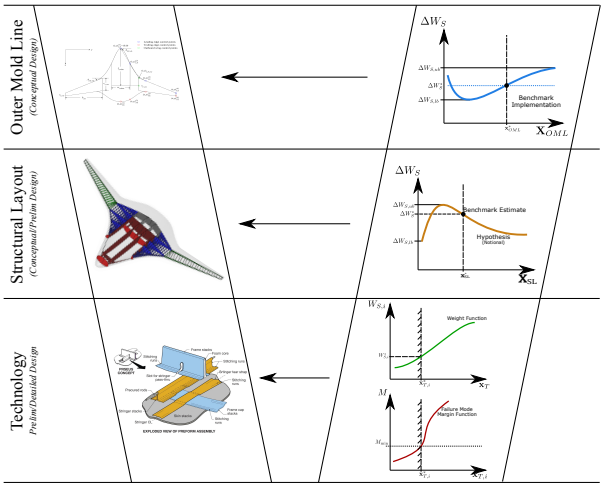

Fig. 3 Hierarchy of structural technology performance characterization

A decomposition of this functional characterization problem is shown in Fig. 3. The top level shows $\mathbf{X}_{OML}$ design space, which directly connects to conceptual design tools. The middle level is the structural layout design space, $\mathbf{X}_{SL}$, which is typically fluid and a source of epistemic uncertainty in the conceptual design phase. However, a definition of $\mathbf{X}_{SL}$ is required for the generation of a global finite element model (GFEM) representation of the aircraft in a physics-based weight estimation process. The lowest level is the technology design space, $\mathbf{X}_T$, or the component level. In physics-based structural weight estimation, these design variables exist for every discrete sizing component in the GFEM, and their values are calculated through a constrained optimization problem, i.e. structural sizing.

Setting up this mapping is the first step in developing a systematic, traceable, and repeatable process to characterize performance for any weight-reducing structural technology. Beginning at the technology level, if the characteristics of structural technology performance, ΔW_S, at a given design space level indicate a potentially significant relationship with the conceptual design space, $\mathbf{X}_{OML}$, then performance should be characterized at the next higher level. There-

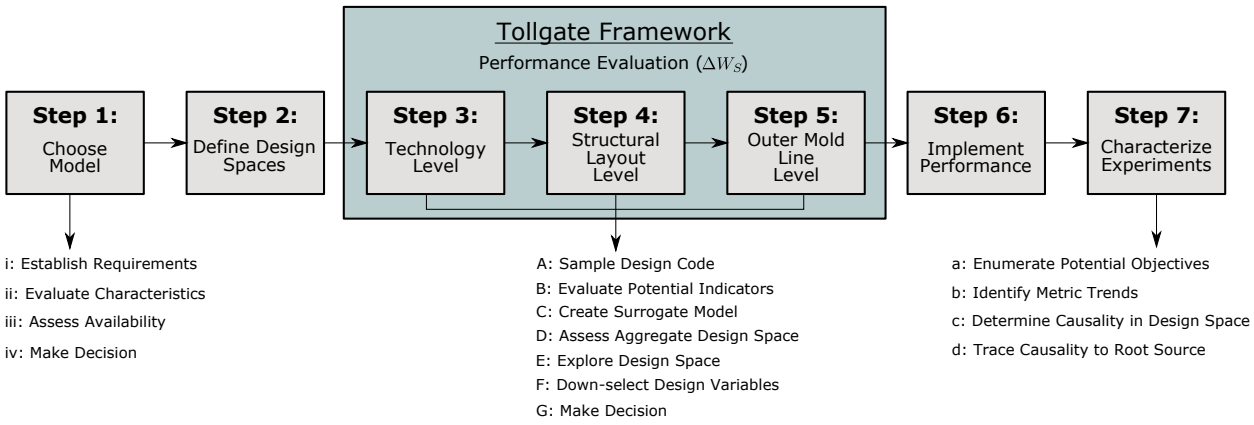

Fig. 4 A tollgate approach for structural technology performance characterization and implementation

fore, evidence supporting or refuting hypotheses at each design space level is built on results generated at the current design space level and all those below it.

This mapping establishes a tollgate formulation for the structural technology to mitigate unnecessary modeling and to generate observations which help decide at each step if moving forward is appropriate. On the right side of Fig. 3, moving up the design space levels requires a significantly larger turnaround time, both in model setup and execution. This mapping also enables traceability and allows for a decoupling of potential effects when moving from one design space level to the next. For example, the impact of structural layout level design variables, $\mathbf{X}_{SL}$, on weight and performance metrics, $W_{S,T}$ or ΔW_S, are the result of a summation of effects from all considered structural components in the entire aircraft. Unless the structural layout is held constant between the baseline configuration and the technology-infused configuration, then single-panel effects cannot be compared between configurations. Additionally, local loading conditions cannot be explicitly controlled in a full aircraft model - they are a function of the global aircraft load cases and structural properties.

The success of this mapping is dependent on the ability to systematically identify whether the conceptual design space has a consequential impact on structural technology performance and, in turn, determine whether that impact introduces risk in conceptual design studies and experiment design for technology development and demonstration. Development of this systematic approach follows a top-down decision support process described in Ref. [11]. This was found to be an appropriate framework because the mapping in Fig. 3 is set up as a series of decision points, e.g. the decision to move forward to a more comprehensive characterization of structural technology performance.

The resulting methodology is shown in Fig. 4, and is described in further detail in Ref. [4]. This approach was used in a functional characterization of the PRSEUS technology, which is described in the following sections.

4 Test Case

For this research, structural technology performance is estimated for the PRSEUS technology on a commercial configuration HWB aircraft. Two baseline OML configurations were considered, NASA's generic HWB301 [13] and the NASA/Boeing N2A [8], and their planforms are shown in Fig. 5. Design space exploration was considered for the latter.

The design space considered for the $\mathbf{X}_{OML}$ and $\mathbf{X}_{SL}$ levels of the mapping is shown in Table 1. A down-selection was performed and it was determined that the outboard wing parameters contributed to a significant amount of variability across all sections of the HWB, e.g. cen-

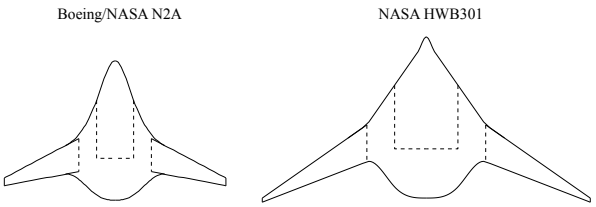

Fig. 5 Boeing/NASA N2A and NASA HWB301 planforms

terbody (cb), rear centerbody (rcb), trapezoidal wing (tw), and outboard wing (ow). To provide a basis of comparison similar to the benchmark technology performance estimation process [19], orthogrid stiffened sandwich composites (12 variables in $\mathbf{X}_{T,B}$) and integrally blade stiffened composites (6 variables in $\mathbf{X}_{T,B}$) were applied to the centerbody and wing sections (tw and ow) of the baseline vehicle ($\mathbf{X}_B$). The same laminate stack was used for both PRSEUS (17 design variables in $\mathbf{X}_{T,T}$) and baseline composite configurations; however, knockdown and non-optimal factors on allowables for strength and stability were appropriately tuned for the PRSEUS concept.

Table 1 OML and structural layout design variables considered for N2A outboard wing

Variable	Description
S	Planform area
AR	Aspect ratio
TR	Taper ratio
Λ_{LE}	Leading edge sweep
c_{FS}	Front spar % chord
c_{RS}	Front spar % chord
p_{rib}	Rib spacing (pitch)

5 Results and Observations

The tollgate process shown in Fig. 4 was followed for this test case. In Step 1, the modeling and simulation environment developed by Laughlin was used [9], and Step 2 was performed for the test case setup in the previous section. At the technology level, a simple non-FEM flat plate was modeled in Collier Research's Hypersizer in order to test different loading scenarios [16]. The two baseline HWB configurations, N2A and HWB301, were used in for the structural layout level.

At the $\mathbf{X}_{OML}$ level, different assumptions regarding the treatment of $\mathbf{X}_{SL}$ were tested. First, an "***Uninformed***" approach kept the same arbitrary structural layout for both the baseline and technology vehicle configuration. A "***Benchmark***" approach was also tested, in which the structural layout was optimized for a baseline OML configuration, $\mathbf{X}_{OML,B}$, and kept constant for both technology and baseline structures throughout the OML design space. Finally, the "***STEED***" treatment, representing the Structural Technology Evaluation for Experiment Design methodology [4], optimized the structural layout for every point in the $\mathbf{X}_{OML,B}$ and $\mathbf{X}_{OML,T}$ for the baseline and technology configurations, respectively. With this approach, enabled by a parametric FEM-based weight estimation framework and surrogate modeling, technology characteristics that enable more efficient structural layouts could be examined.

5.1 Technology Level

The objective of Step 3 was to assess structural technology performance as an aggregate of the technology level design space that was considered. Surrogates were developed for structural weight of each of four panels that were modeled at this level, single panel baseline and technology representations of the centerbody and wing, and performance for the representations of the wing and centerbody were calculated through:

$$\begin{aligned}\Delta W_{S,w} &= W_{S,blade}\left(\mathbf{x}_{T\sim f(OML,SL)}\right) \\ &\quad - W_{S,PRSEUS,w}\left(\mathbf{x}_{T\sim f(OML,SL)}\right) \\ \Delta W_{S,cb} &= W_{S,orthogrid}\left(\mathbf{x}_{T\sim f(OML,SL)}\right) \\ &\quad - W_{S,PRSEUS,cb}\left(\mathbf{x}_{T\sim f(OML,SL)}\right)\end{aligned} \tag{4}$$

respectively, where $\mathbf{x}_{T\sim f(OML,SL)}$ represents the technology level variables that directly map to

the OML and SL design spaces, e.g. component length, component width, and boundary conditions like loads. A 50,000-case Monte Carlo simulation (MCS) was performed with each of the surrogates – $W_{S,blade}$, $W_{S,PRSEUS,w}$, $W_{S,orthogrid}$, and $W_{S,PRSEUS,cb}$ – to represent performance distributions, $\Delta W_{S,w}$ and $\Delta W_{S,cb}$, for the $\mathbf{X}_{T\sim f(OML,SL)}$ design space. The functions represented in Eqn. 4 were generated with cases in which all other variables in $\mathbf{X}_T$ for each structure concept were optimized for weight.

Aggregate results representative of the centerbody concept are shown in Fig. 6 for a flat panel pressure loading condition, P. Each plot shows a set of histograms with these single variable influences. Each histogram shows results from a Monte Carlo simulation with a uniform distribution of a single variable of the corresponding color: Red - panel length, Green - panel width, and Blue - local pressure magnitude. The bounds for each of these variables was $\pm 50\%$ of their nominal values. Each plot represents a different default value of the other two variables in $\mathbf{X}_{T\sim f(OML,SL)}$ corresponding to a percentage level of its respective range above its lower bound: Top - 25% and Bottom - 50%.

The distribution of histograms in Fig. 6 is unique to the bounds placed on the variables in $\mathbf{X}_{T\sim f(OML,SL)}$, and therefore, the following observations are made with these bounds in mind. The first and obvious observation is that the variation of weight reduction performance is decidedly non-zero in each histogram. Any variability in performance as a function of $\mathbf{X}_{T\sim f(OML,SL)}$ warrants investigation of the next level since the technology level is the furthest removed from OML.

Variation in centerbody performance remains relatively consistent for each level of the other defaulted parameters. This trend means that a similar gradient exists for the orthogrid and PRSEUS concepts, i.e. $\partial W_S/\partial x$ for x in $\mathbf{X}_{T\sim f(OML,SL)}$. However, a slight increase in spread of the histograms exists in the bottom plot. Therefore, at higher levels of pressure, there is a greater chance that panel sizes exist in which PRSEUS performance becomes negative, i.e. structural weight is

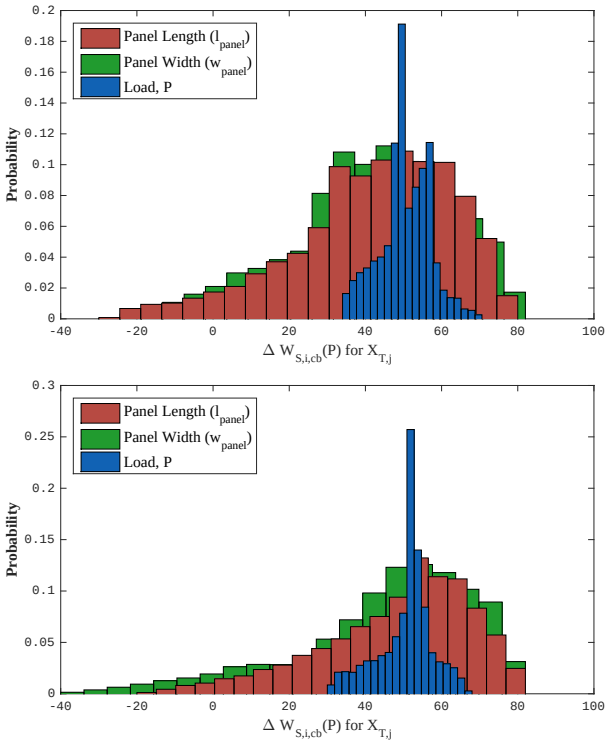

Fig. 6 Effect of panel dimensions on ΔW_S under a panel pressure load

increased by implementing PRSEUS rather than the baseline orthogrid concept. Increased structural weight is likely for smaller panels in which the pressure loading has less of an impact on the maximum bending stresses. This trend is an important consideration for design parameters like centerbody bay width and rib spacing, which define panel dimensions for pressure containing components and have a larger affect on performance variability within the bounds examined.

5.2 Structural Layout Level

A 3-level full factorial design of experiments (DoE) was performed on the structural layout parameters identified in Table 1. While front and rear spar locations are historically defined by considerations for high lift and control devices, it was assumed that an appropriate configuration could be achieved for each design in $\mathbf{X}_{SL}$. Figures 7 and 8 show resulting data from the DoE for the N2A and HWB301 configurations, respectively. Each plot shows front spar and rear spar

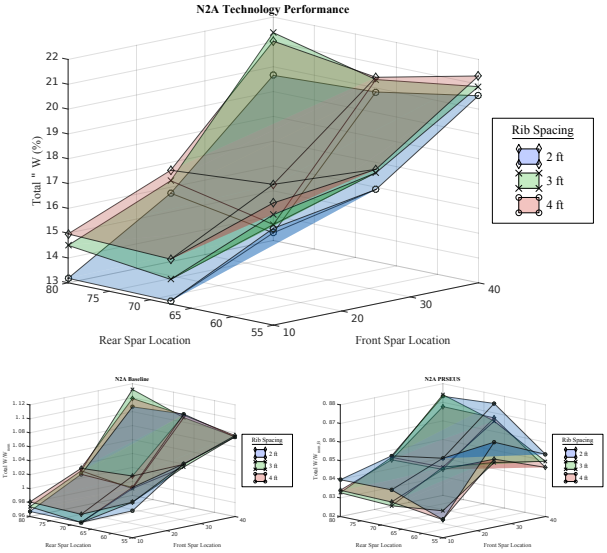

Fig. 7 Total $\Delta W_S\left(\mathbf{X}_{SL} = \mathbf{X}_{SL,B} = \mathbf{X}_{SL,T}\right)$ for N2A configuration enabled by PRSEUS

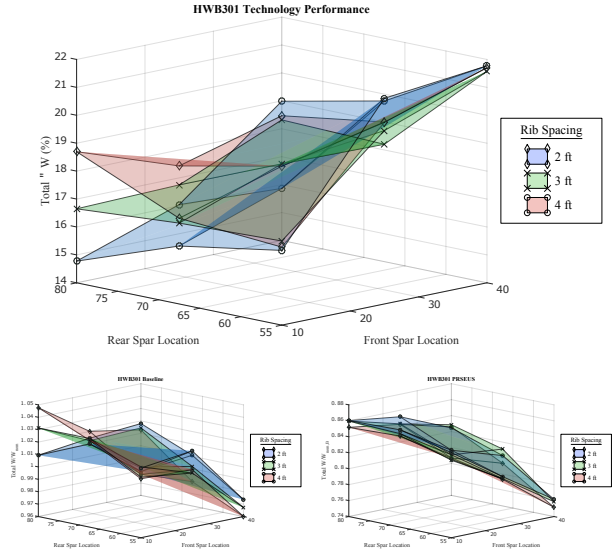

Fig. 8 Total $\Delta W_S\left(\mathbf{X}_{SL} = \mathbf{X}_{SL,B} = \mathbf{X}_{SL,T}\right)$ for HWB301 configuration enabled by PRSEUS

location plotted along the x-axis and y-axis, respectively, and each surface represents a different rib spacing: $p_{\text{rib}} = 2$ ft (blue), $p_{\text{rib}} = 3$ ft (green), and $p_{\text{rib}} = 4$ ft (red). Values of the design variable ranges for this experiment were chosen to reflect the conventional wing structure reviewed in Ref. [18].

For the N2A, the top plot shows a total range of performance from 13.1% structural weight saved by PRSEUS to a potential 21.4%, resulting in a potential difference of 15,207 lbs using the benchmark definition of performance. Weight reduction at the nominal design point was estimated at 16,371 lbs, and therefore, the total range of difference throughout the design space is nearly 67.5% of the benchmark predicted performance value. An error of this magnitude is significant and supports the consideration of variation in structural layout for structural technology performance estimation as a function of the OML.

Performance in the top plot is the direct subtraction of the bottom right plot from the bottom left plot, which show the total structural weight of the PRSEUS and baseline structural concepts, respectively. These plots are normalized by the nominal total baseline structural weight, $W_{S,B}\left(c_{FS} = 25\%,\ c_{RS} = 67.5\%,\ p_{rib} = 3 \text{ ft}\right)$ for ease of comparison. PRSEUS total structural weight, shows a higher degree of nonlinearity in comparison to the baseline, and the surfaces cross at multiple points in the design space, signifying further nonlinearity as a function of rib pitch.

Also noted is the minimum weight design point among any configuration for both baseline and technology-infused N2A aircraft: the PRSEUS configuration with $\mathbf{x}_{SL,T} = [c_{FS} = 10\%,\ c_{RS} = 55\%,\ p_{rib} = 4 \text{ ft}]$. PRSEUS performance for the total aircraft structural weight at this point is $\Delta W_S = 17.9\%$, which shows that *the best structural design does not necessarily correspond to the configuration with best technology performance*. In this case, the technology enabled a better performing structural layout compared to the most optimal baseline configuration of $\mathbf{x}_{SL,B} = [c_{FS} = 10\%,\ c_{RS} = 67.5\%,\ p_{rib} = 2 \text{ ft}]$. Under the assumptions of the model, both configurations seemed to show better performance for the technology and lower structural weight for the entire aircraft at a front spar location of 10% chord.

The other OML design point considered was the HWB301, and the same set of results are shown in Fig. 8. The first observation of the performance surfaces is the separation of surfaces at the region $\mathbf{x}_{SL,T} = [c_{FS} = 10\%, c_{RS} = 80\%]$,

showing nonlinearity in performance as a function of rib spacing. This region is also the set of designs with largest baseline and technology structural weights and the smallest reduction in weight for the PRSEUS technology on the HWB301. The minimum weight solution for the HWB301 exists at the point of greatest PRSEUS performance, a departing trend from the N2A. Using the benchmark approach in this case, so long as topology optimization was performed in designing the structural layout, would generate the same estimate as an approach in which the effort was take to optimize both baseline and technology configurations separately. The differences between the two baselines demonstrate the value of examining $\mathbf{X}_{SL}$ independently of $\mathbf{X}_{OML}$ in the 2nd level of the mapping. These observations help delineate SL performance trends from OML performance trends and make a case for examining the OML space with optimization of the structural layout at each design point, $\mathbf{x}_{OML}$.

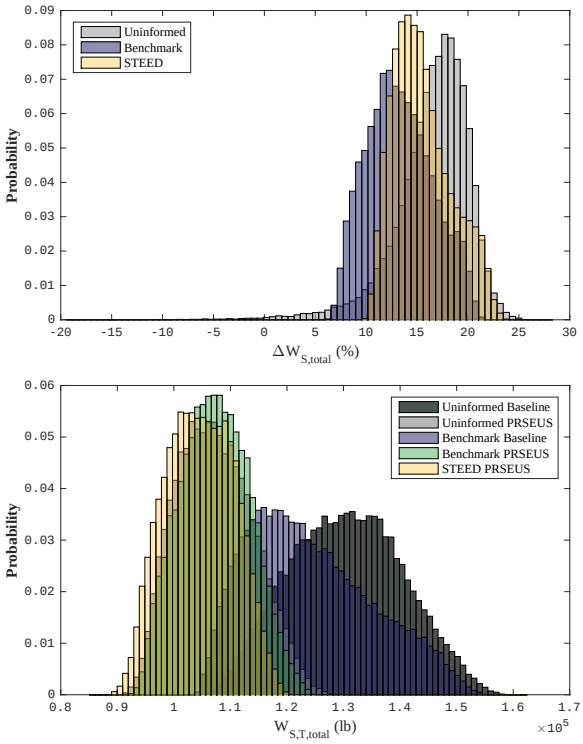

Fig. 9 Technology performance (top) and total structural weights (bottom) in $\mathbf{X}_{OML}$

5.3 Vehicle Level

The last step (Step 5) in the tollgate process shown in Fig. 4 represents the $\mathbf{X}_{OML}$ level in framework mapping. At the beginning of this section, three different treatments of structural layout in the OML design space were described. Figure 9 shows a comparison of the aggregate technology performance (top) and the aggregate structural weights of baseline and PRSEUS configurations (bottom) with the three treatments. The histograms are the result of a 100,000-case MCS of uniformly distributed parameters in $\mathbf{X}_{OML}$ (also $\mathbf{X}_{SL}$ for the "Uninformed" approach) and are shown with transparency for clarity on all distributions.

The top plot shows that an "Uninformed" treatment of the SL comparatively over-predicts performance on average and has a much higher spread on the predicted weight reduction capability of the PRSEUS technology. This treatment is somewhat unrealistic but may be required with limited parametric modeling capabilities. Comparing the "Benchmark" and "STEED" treatments shows that holding the structural layout constant between the baseline and PRSEUS configurations limits the performance of the technology throughout the design space, even though the structural layout has been optimized for the baseline at each design point. Only by optimizing the structural layout for both configurations in the "STEED" treatment was the full weight reduction potential of PRSEUS achieved. This trend is further displayed by the left shift of the "STEED" histogram (yellow) compared to the "Benchmark" (green) in the bottom plot, where each histogram represents a different baseline or PRSEUS structural weight distribution within the design space.

An alternative depiction of PRSEUS performance throughout the OML design space is shown in Fig. 10. Each scatter plot shows PRSEUS performance (y-axis) as a function of the total weight of the PRSEUS configured aircraft. The top plot shows the comparison of the "Uninformed" (grey) vs. "Benchmark" (red) treatments of the structural layout. By optimizing the structural layout for the baseline config-

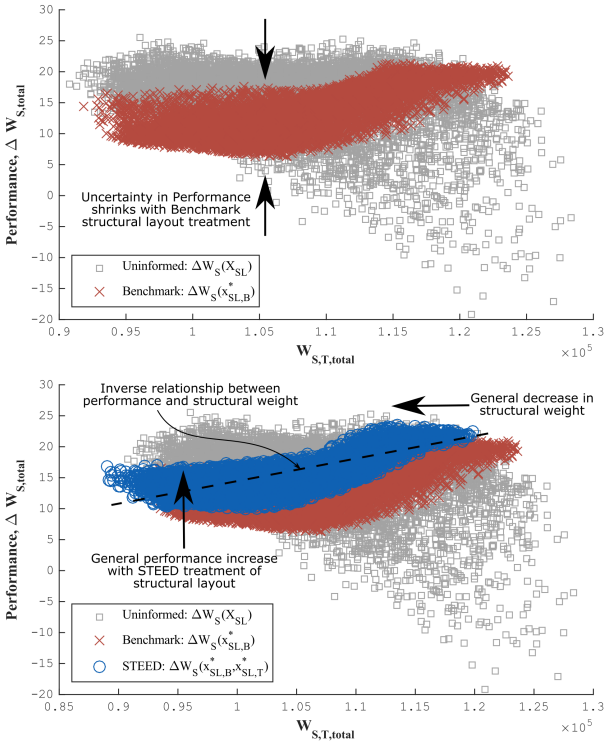

Fig. 10 Technology performance vs. total aircraft structural weight

uration in the "Benchmark" treatment, unrealistic performance estimates are mitigated. If the SL was set arbitrarily for each design point in the OML for both baseline and PRSEUS configurations, it could be interpreted that decreased PRSEUS performance contributes to increased aircraft structural weight. However, the "Benchmark" and consequently "STEED" (bottom plot) treatments of the structural layout show otherwise.

By considering separate optimization of structural layouts for both baseline and technology configurations ("STEED" treatment), it is shown that: 1) structural weight of the aggregate design space is decreased, 2) increased PRSEUS performance does not translate to the minimum weight design in the $\mathbf{X}_{OML}$ space, and 3) there is a general increase in performance throughout the design space, which substantiates the observations from Fig. 9. These observations warranted the "STEED" treatment of the SL in characterization of technology performance, and therefore the weight reduction estimates with

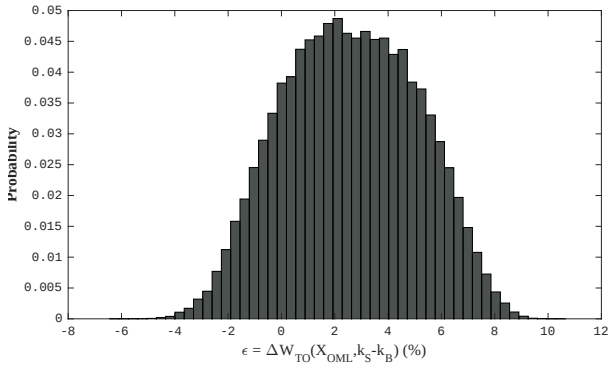

Fig. 11 Error in Benchmark estimates of W_{TO} by neglecting $\Delta W_S \sim f(\mathbf{X}_{OML})$

the STEED approach were fit with a surrogate model: $k_{ST} \sim f(\mathbf{X}_{OML})$, where k_{ST} is defined in Eqn. 2.

This functional PRSEUS performance estimate was implemented in a FLOPS model for the N2A, which was given the same mission and explored different designs in $\mathbf{X}_{OML}$ to assess changes in conceptual design metrics, e.g. fuel burn (W_F), takeoff gross weight (W_{TO}), etc. Figure 11 shows the estimated error in W_{TO} throughout the design space by implementing a scalar PRSEUS performance value and neglecting the functional relationship of performance with the OML.

6 Conclusions

This paper provided an approach for S/RI composite performance estimation that is traceable to the lowest level technology design space. The approach provides insights to the source of technology weight reduction capability and how the technology performs in each level of the design space mapping. This information can be leveraged in the implementation of the technology in conceptual design trade studies, which reduces potential error and risk in aircraft performance estimates. Additionally, the methodology could be used in physical experiment planning for technology development and demonstration to isolate particular phenomena that contribute to uncertainty in technology performance.

References

[1] A. C. Bergan, J. G. J. Bakuckas, A. E. Lovejoy, D. C. Jegley, J. Awerbuch, and T.-M. Tan. Assessment of damage containment features of a full-scale prseus fuselage panel through test and teardown. In *27th ASC Technical Conference*, 2012.

[2] F. Collier, R. Thomas, C. Burley, C. Nickol, C.-M. Lee, and M. Tong. Environmentally responsible aviation: Real solutions for environmental challenges facing aviation. In *27TH INTERNATIONAL CONGRESS OF THE AERONAUTICAL SCIENCES*, 2010.

[3] R. C. J. Combes. Design for damage tolerance. *Journal of Aircraft*, 7:18–20, 1969.

[4] J. A. Corman. *A methodology for structural technology performance characterization to enable reduction of structural uncertainty*. PhD thesis, Georgia Institute of Technology, 2017.

[5] J. A. Corman, N. Weston, C. Friedland, D. N. Mavris, and T. W. Laughlin. Rapid airframe design environment (rade): A parametric, modular, and multidisciplinary framework for conceptual phase aiframe design. In *2018 AIAA Modeling and Simulation Technologies Conference*, page 1930, 2018.

[6] E. Glaessgen, I. Raju, and J. P. C.C. Fracture mechanics analysis of stitched stiffener-skin debonding. In *39th AIAA/ASME/ASCE/AHS/ASC Structures, Structural Dynamics, and Materials Conference and Exhibit*, 1998.

[7] D. C. Jegley and A. Velicki. Status of advanced stitched unitized composite aircraft structures. In *51st AIAA Aerospace Sciences Meeting including the New Horizons Forum and Aerospace Exposition*, 2013.

[8] R. Kawai. Acoustic prediction methodology and test validation for an efficient low-noise hybrid wing body subsonic transport. Technical report, NASA ARMD Subsonic Fixed Wing Project Contract NNL07AA54C, 2011.

[9] T. W. Laughlin. A parametric and physics-based approach to structural weight estimation of the hybrid wing body aircraft. Master's thesis, Georgia Institute of Technology, 2012.

[10] R. Liebeck. Design of the blended wing body subsonic transport. *Journal of Aircraft*, 41:10–25, 2004.

[11] D. N. Mavris, A. P. Baker, and D. P. Schrage. Ippd through robust design simulation for an affordable short haul civil tiltrotor. 1997.

[12] L. McCullers. Flight optimization system, release 6.12, user's guide. NASA, 2004.

[13] C. L. Nickol. Hybrid wing body configuration scaling study. In *50th AIAA Aerospace Sciences Meeting including the New Horizons Forum and Aerospace Exposition*, 2012.

[14] P. Niskode, R. Stickes, B. Allmon, and R. DeJong. Faa cleen consortium open session. *Presentation CLEEN Consortium Open Session, Georgia Institute of Technology, Atlanta, GA, October*, 27, 2010.

[15] M. C.-Y. Niu. *Composite airframe structures: practical design information and data*. Adaso Adastra Engineering Center, 1992.

[16] C. Research. *HyperSizer Rod/Bulb Stiffened Panel Family, User's Manual Edition 5.9*, 2010.

[17] J. S. Schutte and H. Jimenez. Technology assesment of nasa enviromentally responsible aviation advanced vehicle concepts. In *49th AIAA Aerospace Sciences Meeting*, 2011.

[18] M. D. Sensmeier and J. A. Samareh. A study of vehicle structural layouts in post-wwii aircraft. In *45th AIAA/ASME/ASCE/AHS/ASC Structures, Structural Dynamics and Materials Conference*, 2004.

[19] A. Velicki. Damage arresting composites for shaped vehicles: Phase 1 final report. Technical report, NASA/CR-2009-215932, 2009.

Acknowledgments

The authors would like to graciously thank Dr. Fayette Collier, Ms. Dawn Jegley, and Mr. Alex Velicki for their support and guidance with respect to the NASA ERA program and PRSEUS concept.

Contact Author Email Address

jason.corman@gatech.edu

Copyright Statement